Evaluation of drying parameters and sorption isotherms of mint leaves (*M. pulegium*)

C.S. Ethmane Kane[1*], M.A.O. Sid'Ahmed[1] and M. Kouhila[2]

[1] Université de Nouakchott, Faculté des Sciences et Techniques de Nouakchott,
Département de Physique, B.P. 5026, Nouakchott, Mauritanie

[2] Equipe d'Energie Solaire et Séchage des Plantes Médicinales
Ecole Normale Supérieure, B.P. 2400, Marrakech, Maroc

Abstract - *This paper deals with sorption isotherms and drying kinetics of mint leaves (M. pulegium). The sorption isotherms have been determined using a static gravimetric method and then fitted by GAB, equation at 30, 40 and 50 °C over a range of relative humidity from 0.05 to 0.9. Experimental data for the drying of mint was obtained at four temperatures and two flow rate. The increase in air temperature significantly reduced the drying time of the mint leaves. Drying data of this material were analysed to obtain diffusivity values from the falling rate-drying period. In this period, moisture transfer from mint leaves was described by applying the Fick's diffusion model. Effective diffusivity varied from 1.9871×10^{-11} to 1.4221×10^{-10} m²/s and increased with the air temperature. An Arrhenius relation with an activation energy value of 57.12 kJ/mol expressed effect of temperature on the diffusivity. The expression of the drying rate is determined empirically from the characteristic curve of drying. The logarithmic model was found to satisfactorily describe the kinetics of air-drying of mint leaves.*

Résumé - *Cet article présente l'étude des isothermes de sorption et des cinétiques du séchage de la menthe pouliot (M. pulegium). Les isothermes de sorption sont obtenues en utilisant la méthode gravimétrique statique pour les températures 30, 40 et 50 °C sur une gamme d'humidité variant de 0.05 à 0.9. Et les données expérimentales sont modélisées par le modèle de GAB. Les cinétiques de séchage de la menthe sont obtenues pour les températures 40, 50, 60 et 70 °C. L'augmentation de la température d'air chaud a réduit de manière significative la période du séchage des feuilles. Le transfert de l'humidité à partir des feuilles a été décrit en appliquant le modèle de la diffusion de Fick. La diffusivité efficace varie de 1.9871×10^{-11} à 1.4221×10^{-10} m²/s, et elle augmente avec la température de l'air. L'énergie d'activation de la menthe pouliot obtenue à partir de l'équation d'Arrhenius est de 57.12 kJ/mol. L'équation caractéristique du séchage a été déterminée et le modèle logarithmique s'est avéré le plus adéquat pour décrire dans une manière satisfaisante la cinétique des feuilles de menthe pouliot.*

Keywords: Activation energy - CDC - Drying curves - Effective diffusivity - Logarithmic equation - *M. pulegium* - Modelling - Water activity.

1. INTRODUCTION

Mints are generally vigorous, spreading plants that tolerate a wide range of conditions, but thrive where there's abundance of water. They can be highly invasive plants, so caution should be taken in cultivation or it can take over an entire garden.

---

* ottmane6@hotmail.com ; sidahmed@univ-nkc.mr ; kouhila@gmail.com

The most common and popular mints for cultivation are *Mentha pulegium, Mentha viridis* and *Mentha suaveolens* in Morocco. The green leaves have a pleasant warm, fresh, aromatic, sweet flavor with a cool aftertaste. Mint essential oils are used to flavor food, candy, teas, breath fresheners, antiseptic, mouth rines, and toothpast. Mint leaves are used in teas, beverages, jellies, syrups, and ice creams.

Mint essential oil and menthol are extensively used as flavorings in drinks, chewing gum and desserts; see mint candy and mint chocolate. The substances that give the mints their characteristic aromas and flavors are Menthol and the Pulegone. The mint family, Lamiaceae, includes many other aromatic herbs, including most of the more common cooking herbs, including basil, rosemary, sage, oregano and catnip.

In common usage, several other plants with fragrant leaves may be erroneously called a mint. Mint leaves are often used by many campers to repel mosquitoes. It is also said that extracts from mint leaves have a particular mosquito killing capability. However, the only compound scientifically proven to repel mosquitoes is deet. Mint oil is also being used as an environmentally friendly insecticide for its ability to kill some common pests like wasps, hornets, ants and cockroaches. Mint was originally used as a medicinal herb to treat stomach ache and chest pains.

During the middle ages, powdered mint leaves were used to whiten teeth. Mint tea is a strong diuretic. Mint also aids digestion. Menthol from mint essential oil (40 – 90 %) is an ingredient of many cosmetics and some perfumes. Menthol and mint essential oil are also much used in medicine as component of many drugs, and are very popular in aromatherapy. A common use is as an antipruritic, especially in insect bite treatments (often along with camphor). It is also used in cigarettes as an additive, because it blocks out the bitter taste of tobacco and soothes the throat. In order to preserve this seasonal plant, and make it available to consumers during the whole year, it undergoes specific technological treatments; such as drying [1, 2].

Drying provides a very useful preservation. Generally, a part of the mint may be tied in small bundles and hung up, or the leaves and flowering tops spread on a screen and dried in the shade. Drying is one of the oldest methods of food preservation, and it represents a very important aspect of food processing. The main aim of drying products is to allow longer periods of storage, minimise packaging requirements and reduce shipping weights [3].

Solar drying is the most common method used to preserve agricultural products in the world and also Morocco. However, it has some problems related to the contamination with dust, soil, sand particles and insects, and being weather dependent. Also, the required drying time can be quite long. Therefore, the drying process should be undertaken in closed equipments to improve the quality of the final product [4].

This work aims to:

- Study influence of temperature on the adsorption- desorption isotherms of mint (*M. Pulegium*);

- Study the drying kinetics for four temperatures at two air flow rate of mint (*M. Pulegium*);

- Determine the characteristic drying curve (CDC);

- Fit the drying curves with thirteen mathematical models;

- Determine the effective diffusivity and the activation energy.

2. ISOTHERMS OF SORPTION

2.1 Materials and methods

2.1.1 Experimental procedure

All materials used in the experiments were produced in Marrakech (Morocco) and obtained from local markets in Marrakech. Fresh samples were used in desorption experiments. Samples used in adsorption experiments were dried in an oven at 105 °C for 24 h. The adsorption-desorption isotherms were determined by the standard static gravimetric technique.

This method is based on the use of saturated salt solutions to maintain a fixed relative humidity. The salts used were KOH, ($MgCl_2$, $6H_2O$), K_2CO_3, $NaNO_3$, KCl and ($BaCl_2$, $2H_2O$). These salts (**Table 1**) have a range of water activity from 0.05 to 0.9 [5]. The experiment apparatus is shown in Fig. 1.

It consists of six glass jars of 1 litter each with an insulated lid. Each glass jar contains a different salt solution so as to have a water activity that varies from 0.05 to 0.9, and they are immersed in a thermostated water bath adjusted to a fixed temperature for 24 h so as to bring the salt solutions to a stationary temperature.

Duplicate samples each of 0.3 ± 0.001 g for desorption and 0.05 ± 0.001 g for adsorption were weighed and placed into glass jars. The weight recording period was about 4 days. This procedure was continued until the weight was constant. The equilibrium moisture content of each sample was determined by a drying oven whose the temperature was fixed at 105 °C (± 0.1 °C). The time required for equilibrium was three weeks or more depending on water activity and temperature of the bath.

Table 1: Water activities of the saturated salt solutions
at three temperatures used in the experiment [5]

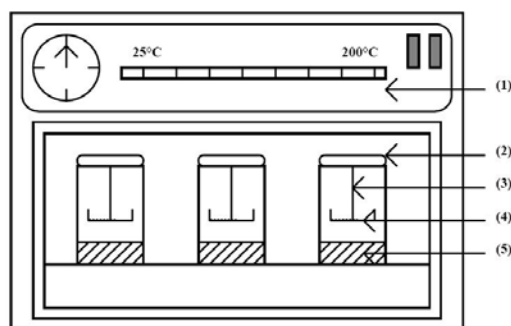| Salt	Water activity		
	30°C	40°C	50°C
KOH	0.0738	0.0626	0.0572
$MgCl_2$, $6H_2O$	0.3238	0.3159	0.3054
K_2CO_3	0.4317	0.4230	0.4091
$NaNO_3$	0.7275	0.7100	0.6904
KCl	0.8362	0.8232	0.8120
$BaCl_2$, $2H_2O$	0.8980	0.8910	0.8823

Fig. 1: Experimental apparatus for the sorption isotherms measurement
(1) Thermostated bath; (2) Glass jar containing salt solution
(3) Sample-holder; (4) Product; (5) Saturated salt solution

2.1.2 The sorption model equations

Experimental moisture sorption data can be described by many sorption models. For the purpose of this work, one isotherm equations were chosen to fit the experimental sorption data; the three parameter GAB model.

The selected equations are detailed in **Table 2**. Nonlinear regression analysis, using the computer programs Curve Expert 3.1, and Origin 6.1, was used to estimate the model coefficients from the experimental sorption data for all samples. The parameters B and C in the GAB equation ({Eq. 1} and {Eq. 2}) can be correlated with temperature using the following Arrhenius-type equation [6, 7].

$$B = B_0 \exp\left(\frac{h_1}{R\,T} \right) \tag{1}$$

$$C = C_0 \exp\left(\frac{h_2}{R\,T} \right) \tag{2}$$

The suitability of the equations has been evaluated and compared between them using the correlation coefficient (r) {Eq. 3}, mean relative error MRE (%) {Eq. 4} and the mean square of error MSE {Eq. 5} [13, 14].

$$r = \sqrt{ \frac{ \sum_{i=1}^{N} \left(M_{pi} - \overline{M}_{ei} \right)^2 }{ \sum_{i=1}^{N} \left(M_{ei} - \overline{M}_{ei} \right)^2 } } \tag{3}$$

$$MRE = \frac{100}{N} \sum_{i=1}^{N} \left| \frac{M_{i,e} - M_{i,p}}{M_{i,e}} \right| \tag{4}$$

$$MSE = \sqrt{ \frac{ \sum_{i=1}^{N} \left(M_{i,e} - M_{i,p} \right)^2 }{ d_f } } \tag{5}$$

Table 2: Equations' describing the moisture sorption isotherms of mint leaves (*M. pulegium*)

Model	Equations	Ref.
GAB	$M = \dfrac{ABC \times a_w}{\left(1 - B \times a_w\right).\left(1 - B \times a_w + BC \times a_w\right)}$ $B = B_0 \exp\left(\dfrac{h_1}{R\,T} \right)$ and $C = C_0 \exp\left(\dfrac{h_2}{R\,T} \right)$	[8]

3. DRYING KINETICS OF *M. pulegium*

3.1 Materials and methods

3.1.1 Solar drying experiments

The experimental apparatus shown in Fig. 2 consisted of a solar dryer, which allows examining the influence of temperature and drying air flow rate on the drying kinetics of product.

It consisted of a solar air collector (dimensions: 2.5 m length, 1 m width), an auxiliary heater, a circulation fan and a drying cabinet (1.4 m length, 0.5 m width, 0.9 m depth and 10 shelves).

The solar collector carried energy of 15500 kWh/m^2/year. The experimental procedure was described in detail by [9].
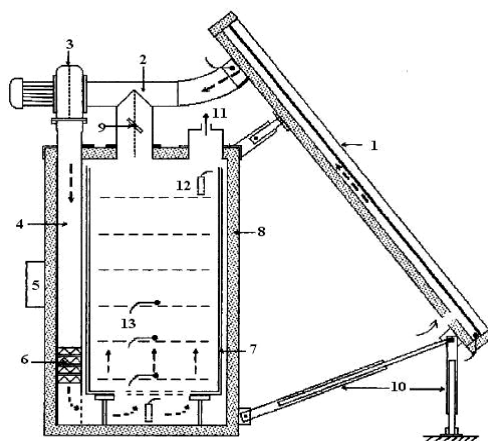

Fig. 2: Schematic representation of the solar dryer
(1) Solar collector; (2) Circulation fan; (3) Fan; (4) Air flow direction, (5) Control box;
(6) Auxiliary heating system; (7) Shelves; (8) Drying cabinet; (9) Recycling air;
(10) Control foot; (11) Exit of air; (12) Humidity probes; (13) Thermocouples

3.1.2 Experimental method

The *M. pulegium* leaves used in the drying experiments were grown in region of Marrakech (31°17'N, 8°W and 463 m of altitude), Morocco. The solar drying experiments were carried out during the period of September and October 2006 in Marrakech. Experiments were performed to determine the effect of the different drying air conditions on the drying kinetics.

Four drying air temperatures (40, 50, 60 and 70°C) and two drying air flow rates (0.028 and 0.056 m^3/s) were selected to examine the influence of temperature and air flow rate on the drying kinetics of the *M. pulegium* leaves. The mass of the *M. pulegium* leaves used in drying experiments was (100.0 ± 0.01) g per tray. The product was uniformly distributed in a single layer on the first shift of the drying cabinet.

Air conditions throughout the experiment were measured and controlled continuously (**Table 3**). Before starting the experiments, the system was run for at least one hour to obtain steady state condition.

Temperature measurements and recording at different points in the solar dryer were made by thermocouples (Chromel-Alumel, 0.2 mm diameter) connected to a data logger enabling ($\pm$ 0.1 °C) accuracy and the outlet temperatures were measured with thermometer.

A digital weighing apparatus ($\pm$ 0.001 g) was used to measure the mass loss of the product. The measurements were made every 10 min at the beginning of the experiment and at 60 min at the end. The initial and final moisture contents of the *M. pulegium* leaves were determined by the oven method (105 °C of 24 h) until the product was completely dehydrated.

Table 3: Drying conditions during experiments
in the solar dryer of mint leaves (*M. pulegium*)

Experiment number	D_v (m^3.s^{-1})	$\theta \pm 0.1$ (°C)	Rh $\pm$ 2 (%)	t (min)
1	0.028	40	51.5	365
2	0.028	50	49.7	225
3	0.028	60	45.5	110
4	0.028	70	42.5	60
5	0.056	40	33.5	257
6	0.056	50	35.4	182
7	0.056	60	38.7	60
8	0.056	70	45.4	40

3.1.3 Mathematical modelling of the solar drying curves

Models have been developed by which the analysis of the drying process of several products and air conditions may be carried out based on only a few laboratory drying experiments [8].

Thus, using [10] of the characteristic drying curve, it is possible to present the drying rate curves of a given product, obtained under different air conditions, by a single normalized drying rate curve. This curve can be used to generalize data for drying kinetics of *M. pulegium* leaves in a convective solar dryer.

Several authors [8], based on the Van Meel transformation, have used simply the initial moisture content (M_0) and the equilibrium moisture content (M_e) to obtain moisture ratio MR {Eq. 6} and initial drying rate $(-dM/dt)_0$ to normalize the drying rate as follows {Eq. 7}:

$$MR = \frac{M - M_e}{M_0 - M_e} \tag{6}$$

$$f = \left(-\frac{dM}{dt}\right)_t / \left(\frac{dM}{dt}\right)_0 \tag{7}$$

where, MR is the moisture ratio and f the dimensionless drying rate.

The solar drying curves obtained were fitted with thirteen different moisture ratio equations (**Table 4**).

Table 4: Mathematical models applied to the drying curves [11]

Model number	Model name	Model expression
1	**Newton**	$MR = \exp(-k \times t)$
2	**Page**	$MR = \exp(-k \times t^n)$
3	**Modified Page1**	$MR = \exp(-(k \times t)^n)$
4	**Modified Page 2**	$MR = \exp((-k \times t)^n)$
5	**Henderson and Pabis**	$MR = a \times \exp(-k \times t)$
6	**Logarithmic**	$MR = a \times \exp(-k \times t) + c$
7	**Two-term**	$MR = a \times \exp(-k_0 \times t) + b \times \exp(-k_1 \times t)$
8	**Two-term exponential**	$MR = a \times \exp(-k \times t) + (1-a) \times \exp(-k \times a \times t)$
9	**Wang and Singh**	$MR = 1 + a \times t + b \times t^2$
10	**Diffusion approach**	$MR = a \times \exp(-k \times t) + (1-a) \times \exp(-k \times b \times t)$
11	**Modified Henderson and Pabis**	$MR = a \times \exp(-k \times t) + b \times \exp(-g \times t) + c \times \exp(-h \times t)$
12	**Verma *et al.***	$MR = a \times \exp(-k \times t) + (1-a) \times \exp(-g \times t)$
13	**Midilli-Kucuk**	$a \times \exp(-k \times t^n) + b \times t$

The correlation coefficient (r^2) was one of the primary criteria for selecting the best equation to define the solar drying curves of *M. pulegium* leaves. In addition to r^2, the statistical parameter, reduced chi-square (χ^2) {Eq. 8}, was used to determine the quality of the fit. This parameter can be calculated as follows:

$$\chi^2 = \frac{\sum_{i=1}^{N} \left(MR_{exp,i} - MR_{pre,i}\right)^2}{N-n} \tag{8}$$

Where $MR_{exp,i}$ is the ith experimental moisture ratio, $MR_{pre,i}$ the ith predicted moisture ratio, N the number of observations, and n the number of constants.

In this study, the coefficients of each model, the most suitable model for drying of *M. pulegium*, the relationship between the drying air temperature and the coefficients of the best suitable model were also determined.

4. RESULTS AND DISCUSSION

4.1 Fitting of sorption models to experimental data

The experimental results for the equilibrium moisture contents of *M. Pulegium*, at each water activity (a_w) for three different temperatures are given in **Table 5** for adsorption and desorption. Equilibrium moisture content data obtained for mint leaves at different water activities and temperatures are shown in figure 4.

Table 5: Equilibrium moisture contents (% d.b.) of mint leaves
(*M. pulegium*) desorption and adsorption data

30 °C			40 °C			50 °C		
H R	des	ads	H R	des	ads	H R	des	ads
0,0738	11,3360	8,3333	0,0626	10,5751	7,6225	0,0572	7,9167	7,0397
0,3238	13,4066	11,8492	0,3159	12,4138	10,2564	0,3054	9,2369	8,9767
0,4317	16,3636	13,6116	0,423	15,0101	12,5227	0,4091	11,6327	11,4130
0,7275	26,4516	20,8333	0,71	25,0000	18,8748	0,6904	18,3333	18,0180
0,8362	31,5789	29,1209	0,8232	30,0866	26,3352	0,812	26,7347	25,9124
0,898	51,7241	46,4151	0,891	45,5399	44,1989	0,8823	44,1860	43,0127
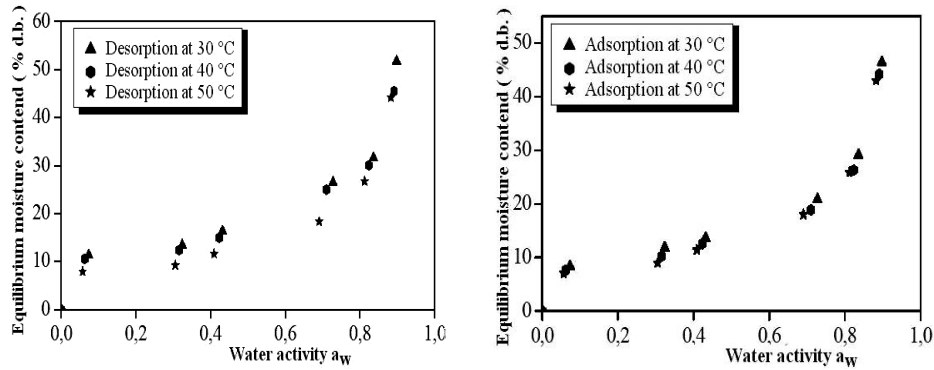
Fig. 3: Influence of temperature on the equilibrium
moisture content of mint leaves (*M. pulegium*)

The sorption isotherms are of sigmoid form (Type II according to the BET classification) which is common for many hygroscopic products. The results reveal the temperature dependence of the sorptive behaviour, with an increase in temperature decreasing the sorption capacity.

Activation of the water molecules due to the increase in temperature causes them to break away from the water binding sites, thus lowering the equilibrium moisture content. The hysteresis phenomenon was observed for the *M. pulegium* (Fig. 4).

The sorption relationships detailed in **Table 2** were fitted to the experimental data for all samples. The results of nonlinear regression analysis of fitting the sorption equations to the experimental data are shown in **Table 6**.

Table 6: Estimated models coefficients, r^2, M R E and M S E fitted
to the sorption isotherms of mint leaves (*M. pulegium*)

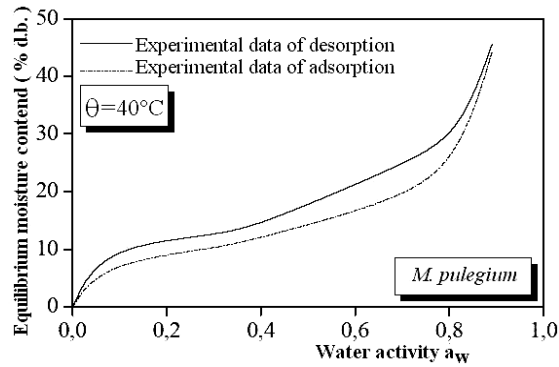| GAB	A	B	C	B_0	C_0
	0.975	1.94E+11	6.065	2.3762	8.923E+18
	h_b	h_c	r^2	MRE (%)	MSE (%)
	-2442,02	-47501,4	0.994	8.498	1.94

Fig. 4: Hysteresis between adsorption and desorption
isotherms for mint leaves (*M. pulegium*)

The moisture content models were compared according to their correlation coefficient (r^2), mean relative error (MRE) and mean square of error (MSE). A model is considered suitable if the MRE value is less than 10 % [12].

GAB equation gave a satisfactory prediction of the adsorption and desorption equilibrium moisture content of all samples. It should be noted that, the goodness of fit of any sorption model to the experimental data shows only a mathematical quality and not the nature of the sorption process [13].

Using these coefficients, the sorption isotherms of *M. pulegium*, are predicted by GAB, equation. The representation of these results is shown in Fig. 5 from which it can be noted that the predicted curve by GAB's model and the experimental data have practically the same rate.

The experiments on the kinetics of drying of mint (*M. pulegium*) were carried out for the period from September to October 2006 with Marrakech, Morocco during the experiments, the temperature of the ambient air with varied from 32 to 42 °C, the humidity relating of the ambient air from 33 to 54 %, the temperature of the draining air from 40 to 70°C and the air flow rate from 0.028 to 0.056 m^3/s.
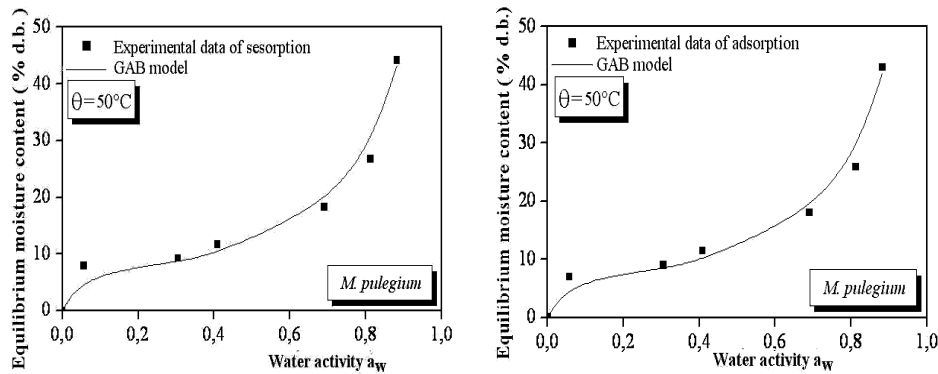

Fig. 5: Experimental and predicted moisture sorption isotherms
of mint leaves (*M. pulegium*) using three empirical models

4.2 Drying curves

These curves are a plot of moisture content against drying time (Fig. 6). It is evident that drying time decreased dramatically as drying temperature was increased from 40 to 70°C and drying air flow rate was increased from 0.028 to 0.056 m³/s.

The drying air conditions have an important influence on the rate of these curves. At constant drying air flow rate (0.028 and 0.056 m³/s), the changes in the drying rate versus moisture content and drying rate versus time are shown in figure 7 and 8 respectively.

It is apparent that drying rate decreases continuously with the moisture content. Drying rate increased with the increase of air-drying temperature and the highest values of drying rate were obtained during the experiment at 70 °C of the drying air. The results were generally in agreement with some literature studies on drying of various food products [14].

In general, the time required to reduce the moisture ratio to any given level was dependent on the drying condition, being the highest at 40 °C and the lowest at 70 °C. Similar results were reported by [1, 15].
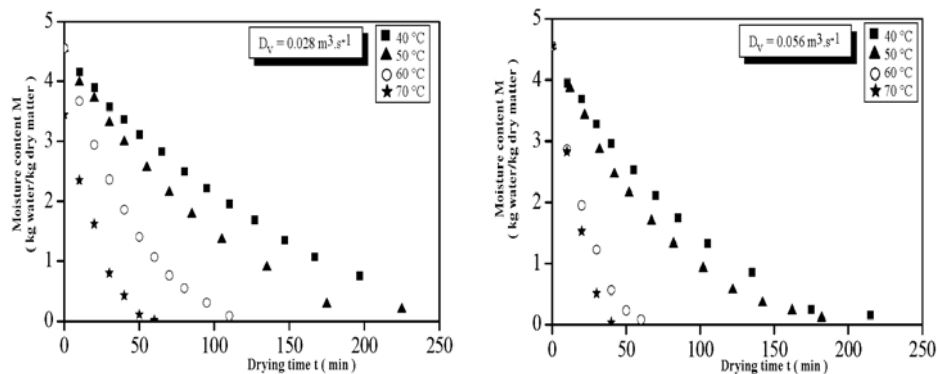

Fig. 6: Variation of moisture content as a function of time for different
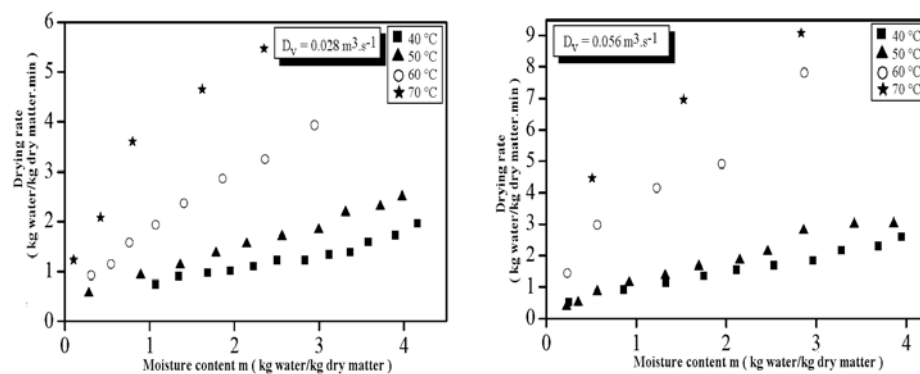drying air conditions of mint leaves (*M. pulegium*)

Fig. 7: Variations of drying rate as a function of moisture content for
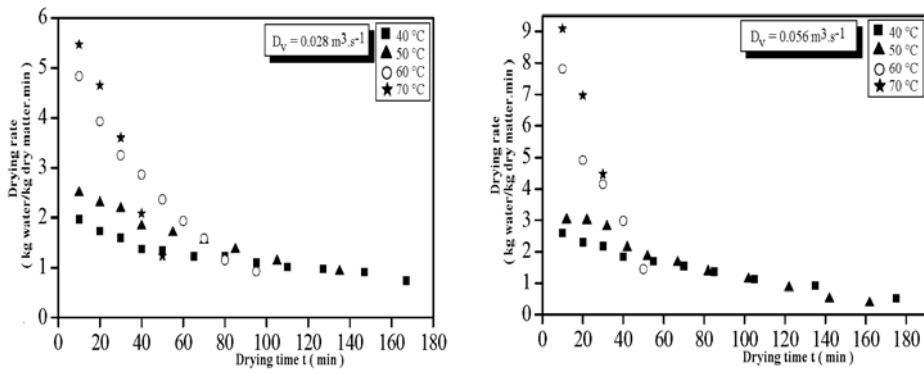different air- drying temperature of mint leaves (*M. pulegium*)

Fig. 8: Variations of drying rate as a function of drying time for
different air- drying temperature of mint leaves (*M. pulegium*)**4.3 Characteristic drying curve**

The change in the moisture ratio versus dimensionless drying rate f are given in figure 9, shows that all solar drying curves obtained for the different tested conditions, fall into a tight band, indicating that the effect of variation in different conditions is small over the range tested.

A polynomial model was found to fit the best the dimensionless experimental data of the *M. pulegium*.
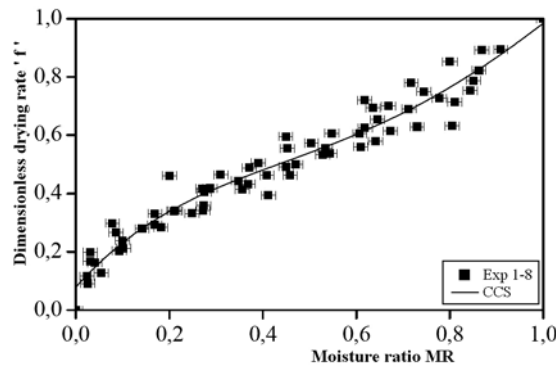
Fig. 9: Characteristic drying curve of mint leaves (*M. pulegium*)

The criterion used to evaluate goodness of fit was the standard error (S_r = 0.0506) and the correlation coefficient (r^2 = 0.9515), {Eq. 9}.

$$f = 0.0545 + 2.7574.MR - 10.1434.MR^2$$
$$+ 22.315.MR^3 - 22.7176.MR^4 + 8.7548.MR^5 \tag{9}$$

4.4 Fitting of the drying curves

The moisture ratio values were fitted against the drying time for the thirteen models. Drying models coefficients were determined (**Table 7**) for 0.028 m³/s and (**Table 8**) for

0.056 m³/s. Moisture ratio models were compared according to their correlation coefficient (r^2) and reduced chi-square (χ^2), which varied between 0.9811 and 0.9999, 8.912×10^{-3} and 1.8×10^{-5}, respectively.

Table 7: Modelling of moisture ratio according to drying time for mint leaves
(*M. pulegium*) for an air flow rate equal to 0.028 m³s⁻¹

Model	θ	Coefficient	r^2	χ^2
Newton	40	$k = 0.0084$	0.9961	0.0006
	50	$k = 0.01211$	0.9932	0.00146
	60	$k = 0.0251$	0.9954	0.00068
	70	$k = 0.0470$	0.9891	0.00292
Page	40	$k = 0.0053$; $n = 1.0997$	0.9977	0.00035
	50	$k = 0.0060$; $n = 1.1637$	0.9849	0.0008
	60	$k = 0.0131$; $n = 1.1706$	0.9988	0.0002692
	70	$k = 0.0172$; $n = 1.322$	0.9970	0.001064005
Modified Page 1	40	$k = 0.00089$; $n = 0.9437$	0.9961	0.000243397
	50	$k = 0.0108$; $n = 1.1159$	0.9932	0.0016068
	60	$k = 0.0153$; $n = 1.6362$	0.9954	0.000657077
	70	$k = 0.0181$; $n = 2.5891$	0.9891	0.003895832
Modified Page 2	40	$k = 0.0085$; $n = 1.0998$	0.9978	0.002432408
	50	$k = 0.0122$; $n = 1.1638$	0.9966	0.000802187
	60	$k = 0.0247$; $n = 1.1706$	0.9988	0.0002692
	70	$k = 0.0463$; $n = 1.3220$	0.9970	0.001063104
Henderson and Pabis	40	$a = 1.0122$; $k = 0.0085$	0.9963	0.000244434
	50	$a = 1.0221$; $k = 0.0125$	0.9937	0.001445796
	60	$a = 1.0278$; $k = 0.0258$	0.9960	0.000970713
	70	$a = 1.0251$; $k = 0.0481$	0.9898	0.00343675
Logarithmic	40	$a = 1.3009$; $k = 0.0054$; $c = -0.3161$	0.9996	0.0000416145
	50	$a = 1.1630$; $k = 0.0091$; $c = -0.1684$	0.9987	0.000294215
	60	$a = 1.1622$; $k = 0.0189$; $c = -0.1612$	0.9999	0.0000272679
	70	$a = 1.4647$; $k = 0.0249$; $c = -0.4647$	0.9986	0.000775
Two term	40	$a = 5.0099$; $k_0 = 0.0152$; $b = -4.1089$; $k_1 = 0.0174$	0.9986	0.00497
	50	$a = 5.1884$; $k_0 = 0.0062$; $b = -4.1962$; $k_1 = 0.0052$	0.9988	0.000297

	60	$a=5.02$; $k_0=0.0131$; $b=-4.0208$; $k_1=0.01103$	0.9999	0.00078
	70	$a=5.0526$; $k_0=0.0169$; $b=-4.0531$; $k_1=0.01211$	0.9985	0.00151
Two term Exponential	40	$a=1.6024$; $k=0.0109$	0.4611	0.000283
	50	$a=1.6755$; $k=0.0163$	0.9969	0.000742
	60	$a=1.0024$; $k=0.02505$	0.9954	0.00107
	70	$a=0.9834$; $k=0.0459$	0.9888	0.00398
Wang and Singh	40	$a=-0.0069$; $b=1.3209$	0.9987	0.0002
	50	$a=-0.0093$; $b=2.2045$	0.9985	0.00036
	60	$a=-0.0192$; $b=9.6792$	0.9993	0.00016
	70	$a=-0.0069$; $b=0.0003$	0.9987	0.000455
Diffusion Approach	40	$a=3.9817$; $k=0.0028$; $b=0.5275$	0.9969	8.12E-04
	50	$a=5.6421$; $k=0.0063$; $b=0.8564$	0.9988	2.97E-04
	60	$a=10.7757$; $k=0.0126$; $b=0.9276$	0.9993	1.80E-05
	70	$a=13.6084$; $k=0.0154$; $b=0.8931$	0.9986	7.56E-04
Modified Henderson and Pabis	40	$a=0.1938$; $k=0.0085$; $b=0.6246$; $g=0.0085$; $c=0.1938$; $h=0.0125$	0.9963	8.48E-04
	50	$a=0.2769$; $k=0.0124$; $b=0.4771$; $g=0.01239$; $c=0.2676$; $h=0.0125$	0.0504	2.42E-03
	60	$a=0.28011$; $k=0.0258$; $b=0.4676$; $g=0.0258$; $c=0.28011$; $h=0.0258$	0.9960	1.64E-03
	70	$a=0.2650$; $k=0.0473$; $b=0.4771$; $g=0.0485$; $c=0.2828$; $h=0.0481$	0.9898	0.005166746
Verma *et al.*	40	$a=2.3727\times10^5$; $k=0.008$; $g=0.0079$	0.4581	6.63E-04
	50	$a=0.1997\times10^5$; $k=0.0074$; $g=0.0074$	0.9975	6.56E-04
	60	$a=1.0262\times10^5$; $k=0.007$; $g=0.0069$	0.99409	1.13E-03
	70	$a=0.21559$; $k=0.00654$; $g=0.0065425$	0.994686	0.002862538
Midilli and Kucuk	40	$a=0.9972$; $k=0.0094$; $b=-0.00108$; $n=0.8944$	0.9998	3.3999E-05
	50	$a=0.9834$; $k=0.00725$; $b=-0.0004$; $n=0.8944$	0.9986	0.000344251
	60	$a=0.99815$; $k=0.0185$; $b=-0.0008$; $n=1.04298$	0.9999	3.40962E-05

	70	$a = 0.9986$; $k = 0.0283$, $b = -0.0041$; $n = 1.06101$	0.9985	0.001530314

Table 8: Modelling of moisture ratio according to drying time for mint leaves
(*M. pulegium*) for an air flow rate equal to 0.056 $m^3 s^{-1}$

Model	θ	Coefficient	r^2	χ^2
Newton	40	$k = 0.01224$	0.9932	0.00146454
	50	$k = 0.0159$	0.9956	0.0044876
	60	$k = 0.0492$	0.9944	0.001453164
	70	$k = 0.0606$	0.9883	0.003695527
Page	40	$k = 0.0063$; $n = 1.1520$	0.9962	0.000903895
	50	$k = 0.0159$; $n = 1.1569$	0.9989	0.000255991
	60	$k = 0.0481$; $n = 1.1476$	0.9964	0.00117757
	70	$k = 0.0592$; $n = 1.4107$	0.9981	0.000874631
Modified	40	$k = 0.0124$; $n = 1.1521$	0.9962	0.000902864
Page 1	50	$k = 0.012$; $n = 1.1327$	0.9956	0.000995878
	60	$k = 0.0215$; $n = 2.2363$	0.9945	0.001816455
	70	$k = 0.0232$; $n = 2.6169$	0.9883	0.005543291
Modified	40	$k = 0.0227$; $n = 0.5395$	0.9932	0.00159107
Page 2	50	$k = 0.0159$; $n = 1.1569$	0.9989	0.000262921
	60	$k = 0.0481$; $n = 1.1476$	0.9964	0.00117757
	70	$k = 0.0592$; $n = 1.4107$	0.9981	0.000877521
Henderson	40	$a = 1.0185$; $k = 0.0125$	0.9935	0.001498449
and Pabis	50	$a = 1.03235$; $k = 0.0165$	0.9964	0.000711876
	60	$a = 1.0114$; $k = 0.0498$	0.9946	0.001743698
	70	$a = 1.0216$; $k = 0.0619$	0.9888	0.00505841
Loga-	40	$a = 1.1765$; $k = 0.0088$; $c = -0.1881$	0.9989	0.000228703
rithmic	50	$a = 1.1315$; $k = 0.0128$; $c = -0.169$	0.9997	6.55425E-05
	60	$a = 1.1603$; $k = 0.0356$; $c = -0.169$	0.9990	0.000417143
	70	$a = 1.677$; $k = 0.0266$; $c = -0.677$	0.9984	0.004913402
Two term	40	$a = 0.7604$; $k_0 = 0.0125$; $b = 0.2581$; $k_1 = 0.0125$	0.9935	0.001442667
	50	$a = 4.9128$; $k_0 = 0.0246$; $b = -3.9195$; $k_1 = 0.0279$	0.9991	0.000240731
	60	$a = 4.8663$; $k_0 = 0.0245$; $b = -3.8764$; $k_1 = 0.0204$	0.9987	0.000699168

	70	$a=4.8533$; $k_0=0.0182$; $b=-3.8539$; $k_1=0.0115$	0.9989	0.000468872
Two term	40	$a=1.6594$; $k=0.0163$	0.9965	0.000759712
Exponential	50	$a=1.6719$; $k=0.0212$	0.6719	0.000247864
	60	$a=1.6297$; $k=0.0627$	0.506	0.001166958
	70	$a=1.9568$; $k=0.0933$	0.9974	0.001229514
Wang and	40	$a=-0.0094$; $b=2.2578\times10^{-5}$	0.9980	0.000506845
Singh	50	$a=-0.0123$; $b=3.9537$	0.9986	0.000316627
	60	$a=-0.0362$; $b=0.0003$	0.9970	0.00097734
	70	$a=-0.0429$; $b=0.0004$	0.9999	2.2707E-05
Diffusion	40	$a=4.1330$; $k=0.0065$; $b=0.7966$	0.9989	0.000300567
approach	50	$a=3.7727$; $k=0.0091$; $b=0.8065$	0.9998	0.004467255
	60	$a=-3.8427$; $k=0.0212$; $b=0.1970$	0.9988	0.00053692
	70	$a=3.0339$; $k=0.0205$; $b=0.4310$	0.9999	6.41651E-06
Modified Henderson and Pabis	40	$a=0.2946$; $k=0.0126$; $b=0.4600$; $g=0.0126$; $c=0.2638$; $h=0.0124$	0.9935	0.002342383
	50	$a=0.2782$; $k=0.0166$; $b=0.4760$; $g=0.0165$; $c=0.2782$; $h=0.0166$	0.9964	0.00088951
	60	$a=0.3157$; $k=0.0497$; $b=0.3799$; $g=0.05$; $c=0.3257$; $h=0.0497$	0.9874	0.008490818
	70	$a=0.3375$; $k=0.0616$; $b=0.3466$; $g=0.0624$; $c=0.3375$; $h=0.0616$	0.9888	0.007345
Verma	40	$a=51.8402$; $k=0.008$; $g=0.00799$	0.9968	0.001186576
et al.	50	$a=2.3517\times10^5$; $k=0.008$; $g=0.00779$	0.9997	6.71671E-05
	60	$a=0.2188\times10^5$; $k=0.0075$; $g=0.0075$	0.9811	0.008912332
	70	$a=0.5439\times10^5$; $k=0.007$; $g=0.00699$	0.9977	0.001961094
Midilli and Kucuk	40	$a=0.9856$; $k=0.0089$; $b=-0.0005$; $n=1.0345$	0.9989	0.000284674
	50	$a=0.9894$; $k=0.0115$; $b=-0.0004$; $n=1.0544$	0.9997	0.000274345
	60	$a=0.9995$; $k=0.06119$; $b=-0.0039$; $n=$;	0.9996	0.000444844
	70	$a=0.9999$; $k=0.368$, $b=-0.0084$; $n=1.0004$	0.9988	0.000202734

The model with the highest (r^2) value and the lower (χ^2) was chosen for best describing the drying curves.

The Logarithmic model showed the best agreement with the experimental data and gave the best results for the drying of mint leaves (*M. pulegium*). Therefore, this model was selected to represent the thin layer, forced convection solar drying behavior of mint leaves (*M. pulegium*) with an r^2 of 0.9999 and χ^2 of 1.8×10^{-5}.

Plots of the predicted moisture ratios with experimental moisture ratios are shown in Fig. 10, it can be seen that the proposed model provided a good agreement between experimental and predicted moisture ratio, which was banding around at 45° straight line.
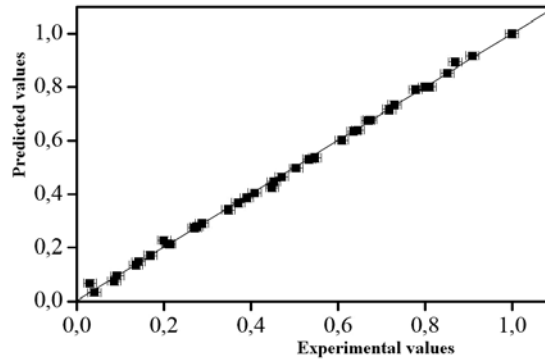

Fig. 10: Experimental and predicted Logarithmic model moisture ratio values
for different drying air conditions of mint leaves (*M. pulegium*)

To take into account the effect of the drying air temperature on the drying coefficients of the Logarithmic equation {Eq. 10}, the values of k and n were correlated for the mint leaves (*M. pulegium*) by the following equations {Eqs. 11-13}, which resulted in the best correlation (r^2 values) among several investigated expressions.

$$M R \ = \ a \times \exp\left(-k \times t\right) + c \tag{10}$$

$$a \ = \ -70.132 + 4.2811\,T - 0.0835\,T^2 + 5.2785\,T^3 \tag{11}$$

$$k \ = \ 12.1566 - 0.7205\,T + 0.0139\,T^2 - 8.67 \times 10^{-5}\,T^3 \tag{12}$$

$$c \ = 1.0961 - 0.1322\,T + 0.0036\,T^2 - 2.84 \times 10^{-5}\,T^3 \tag{13}$$

The relationship between the coefficients of Logarithmic model and the air drying temperature was very significant, with an r^2 of 1 and S_r of 0.

These results can be noted consequently from Fig. 11, which compares experimental data with predicted Logarithmic model values at different air drying temperatures. Accordingly, it can be concluded that the Logarithmic drying model described adequately the drying behavior of *M. pulegium* in the convective solar drying process at a drying air temperature range 40-70°C and drying air flow rates (0.028 and 0.056 m^3/h).
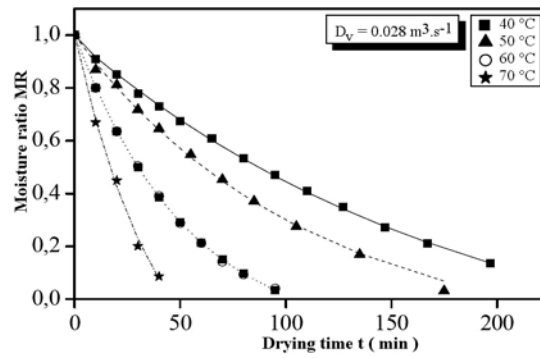
Fig. 11: Influence of drying air temperature on moisture ratios predicted
By Logarithmic model of mint leaves (*M. pulegium*)

4.5 Determination of effective diffusivities

Experimental results can be understood by Fick's diffusion equation. The analytical solution of Fick's second law, developed by [16], in slab geometry by assuming uniform initial moisture distribution, with the simplification of the moisture movement by diffusion, negligible shrinkage, constant diffusion coefficients and temperature can be expressed as {Eq. 14}

$$MR = \frac{8}{\pi^2} \sum_{n=0}^{\infty} \frac{1}{(2n+1)^2} \exp\left(\frac{-(2n+1)^2 \pi^2 D_{eff} t}{4L^2} \right) \qquad (14)$$

where D_{eff} is the effective diffusivity (m^2/s), L is the half thickness of slab (m) for drying from both sides and the thickness of slab (m) for drying from one sides, and $n =$ 1, 2, 3…the number of terms taken into consideration.

For long drying periods, $MR < 0.6$, the equation {Eq. 15} can be simplified to the first term/part of the series only [17]. So, taking a natural logarithm in both members the result is the following

$$Ln(MR) = Ln\left(\frac{8}{\pi^2} \right) - \left(\frac{\pi^2 D_{eff} t}{4L^2} \right) \qquad (15)$$

The diffusion coefficient for each drying temperature was calculated by substituting the experimental data in the previous equation.

The diffusion coefficient is determined by plotting experimental drying data in terms of $\ln(MR)$ versus drying time. From {Eq. 16} a plot of $\ln(MR)$ versus drying time gives a straight line with a slope of

$$k = \frac{\pi^2 \times D_{eff}}{4 L^2} \qquad (16)$$

This slope is the measure of the diffusivity. Figure 12 shows the plot of $\ln(MR)$ versus drying time for the studied range of temperatures. Values of D_{eff} for different temperatures are presented in **Table 9**.

The effective diffusivities of dried samples of sludge at 40-50-60-70 °C vary in the range of 1.9871×10^{-11} to 1.4221×10^{-10} m²/s. The values of D_{eff} increased notably with increasing temperature.

These values are comparable with some others reported in the literature: $2 - 4.2 \times 0^{-10}$ m²/s for drying garlic slices in temperature range of 50 - 90 °C [17], drying of green beans $2.641 – 5.711 \times 10^{-9}$ m²/s in temperature range of 50–70 °C [18], drying of okra $4.27 \times 10^{-10} - 1.30 \times 10^{-9}$ m²/s in temperature range of 50–70°C [19].
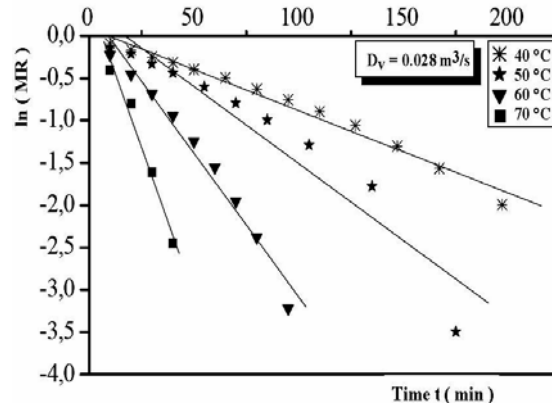

Fig. 12: Experimental and predicted logarithmic moisture ratio at different drying temperatures, $D_V = 0.028 \, m^3 / s$ of mint leaves (*M. pulegium*)

Table 9: Values of effective diffusivity obtained for mint leaves (*M. pulegium*) at different temperatures and $D_V = 0.028 \, m^3 / s$

Temperature (°C)	Effective diffusivity (D_{eff})
40	1.9871×10^{-11}
50	4.2059×10^{-11}
60	6.935×10^{-11}
70	1.4221×10^{-10}

4.6 Activation energy

Effective diffusivity can be related with temperature by Arrhenius expression [16, 19] like {Eq. 17}:

$$D_{eff} = D_0 \times \exp\left(-\frac{E_a}{R(T + 273.15)} \right) \qquad (17)$$

Where, D_0 is the constant in Arrhenius equation (m²/s), E_a is the activation energy (kJ/mol), T is temperature of air (°C) and R is the universal gas constant (kJ/mol.K) {Eq. 18} can be rearranged in the form of:

$$Ln\left(D_{eff}\right) = Ln\left(D_0\right) - \frac{E_a}{R\left(T + 273.15\right)} \tag{18}$$

Values of D_{eff} calculated {Eq. 15} for experiments are plotted figure 13. The plot was found to be essentially a straight line in the range of temperatures investigated, indicating Arrhenius dependence. From the slope of the straight line described by the Arrhenius equation, the activation energy was found to be 57, 12 kJ/mol.

The comparison with literature values for various vegetables is shown in **Table 10**. It is higher than the activation energy of carrot drying [20], red pepper drying [21], green bean drying [22], and green pea drying [23] and lower than the activation energies of mint leaves [1, 2], and black tea drying [24].
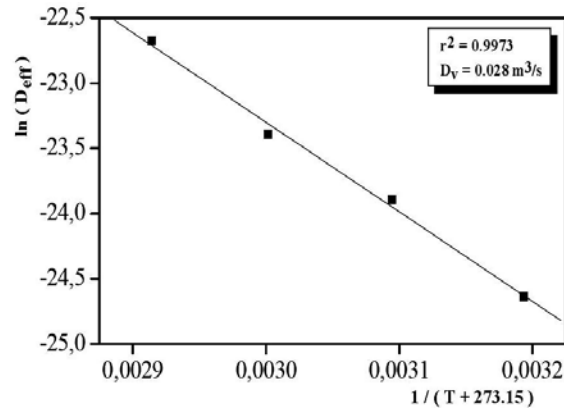

Fig. 13: Influence of air temperature on the
effective diffusivity of mint leaves (*M. pulegium*)

Table 10: Comparison of activation energy values with literature values

Material	Activation energy E_a (kJ/mol)	Ref.
Mint (*M. pulegium*)	57.12	Present work
Mint (*M. spicata* L.)	62.96	[1]
Mint (*M. crispa* L.)	82.93	[2]
Carrot	28.36	[20]
Red pepper	42.8	[21]
Green pea	24.70	[23]
Black tea	406.02	[24]

5. CONCLUSION

The sorption isotherms of mint leaves (*M. pulegium*) have been determined by experiment and then described by GAB model. The saturated salt method can be used successfully for experimental determination of the equilibrium moisture content of mint.

The experimental results show that the sorption isotherms of mint, take a form of the sigmoid type and that GAB model give a better fit for the sorption isotherms of aromatic and medicinal herbs. Desorption values are higher than those for adsorption.

The thin layer solar drying of mint leaves (*M. pulegium*) was investigated in a convective solar dryer with an auxiliary heating system. From the drying kinetics experiments, it was observed that only the falling drying rate period existed and the drying air temperature was the main factor influencing the drying kinetics.

The drying rate increased respectively with the increase of the drying air temperature and the drying air flow rate. The characteristic drying curve was determined and was used to generalize data for drying kinetics of this product.

The values of calculated effective diffusivity for drying at 40 °C, 50 °C, 60 °C and 70 °C of air temperature and 0.028 m^3/s of air flow rate ranged from 1.9871×10^{-11} to 1.4221×10^{-10} m^2/s. The effective diffusivity increases as air temperature.

The activation energy calculated using the Arrhenius type equation, as a function sample temperature during drying, presented 57.12 kJ/mol. Logarithmic's empirical model showed a good fit for all curves.

NOMENCLATURE

A, B, C, D, a, b, c, g, h :
    Model coefficients

ads : Adsorption

des : Desorption

a_w : Water activity

d.b : Dry basis

B_0, C_0, h_1, h_2 : GAB coefficients

CDC: Characteristic drying c urve

L : Slice half thickness (mm)

f : Dimensionless drying rate

k : Slope

d_f : Number of degrees of freedom

d_v : Drying air flow rate (m^3/s)

Exp : Experiment

S_r : Standard error

T : Absolute temperature (K)

r^2 : Correlation coefficient

M : Moisture content at any time of
    Drying (kg water / kg dry matter)

M_e : Equilibrium moisture content (%db)

$M_{i,e}$: i^{th} experimental equilibrium
    moisture content (%db)

$M_{i,p}$: i^{th} predicted equilibrium
    moisture content (%db)

$M R$: Moisture ratio

MRE : Mean relative error (%)

MSE : Mean square error (%)

M_0 : Initial moisture content
    (kg water / kg dry matter)

N : Number of data points

R : Universel gas constant (J/mol/K)

Ln : Logarithm neperien

Rh : Relative humidity

t : Drying time (min)

χ^2 : Reduced chi-square

θ : Temperature (°C)

M. pulegium: *Mentha pulegium*

REFERENCES

[1] I. Doymaz, '*Thin- Layer Drying Behaviour of Mint Leaves* (*Mentha spicata* L.)', Journal of Food Engineering, Vol. 74, N°3, pp. 370 – 375, 2006.

[2] K.J. Park, Z. Vohnikova and F.P.R. Brod, '*Evaluation of Drying Parameters and Desorption Isotherms of Garden Mint Leaves (Mentha crispa. L)*', Journal of Food Engineering, Vol. 51, N°3, pp. 193 – 199, 2002.

[3] M.R. Okos, G. Narsimhan, R.K. Singh and A.C. Weitnauer, '*Food Dehydration*', in Handbook of Food Engineering, D.R. Heldman and D.B. Lund (Eds), pp. 563 – 620, Marcel Dekker, NY, 1992.

[4] C. Ertekin and O. Yaldiz, '*Drying of Eggplant and Selection of a Suitable Thin Layer Drying Model*', Journal of Food Engineering, Vol. 63, N°3, pp. 349 – 359, 2004.

[5] L. Greenspan, '*Humidity Fixed Points of Binary Saturated Aqueous Solutions*', Journal of Research of the National Bureau of Standards, Vol. 81a, pp. 89-112, 1977.

[6] A. Jamali, M. Kouhila, L. Aït Mohamed, J.T. Jaouhari, A. Idlimam and N. Abdenouri, '*Sorption Isotherms of Chenopodium ambrosioïdes Leaves at Three Temperatures*', Journal of Food Engineering, Vol. 72, pp. 77 - 84, 2006a.

[7] A. Jamali, M. Kouhila, L. Aït Mohamed, A. Idlimam and A. Lamharrar, '*Moisture Adsorption-Desorption Isotherms of Citrus reticulata Leaves at Three Temperatures*', Journal of Food Engineering, Vol. 77, N°1, pp. 71 - 78, 2006b.

[8] C. Van Den Berg, '*Development of B.E.T. Like Models for Sorption of Water on Foods; Theory and Relevance*',. In D. Simatos and J.L. Multon (Eds), Properties of Water in Foods, pp. 119 – 135, Dordrecht: Martinus Nijhoft Publishers, 1985.

[9] S. Lahsasni, M. Kouhila, M. Mahrouz and J.T. Jaouhari, '*Drying Knetics of Prickly Pear Fruit (Opuntia ficus indica)*', Journal of Food Engineering, Vol. 61, N°2, pp. 173-179, 2003.

[10] D.A. Van Meel, '*Adiabatic Convection Batch Drying with Recirculation of Air*', Chemical Engineering Science, Vol. 9, N°1, pp. 36 - 44, 1958.

[11] A. Midilli, H. Kucuk and Z. Yapar, '*A New Model for Single Layer Drying*', Drying Technology, Vol. 20, N°7, pp. 1503 - 1513, 2002.

[12] C.J. Lomauro, A.S. Bakshi and T.P. Labuza, '*Evaluation of Food Moisture Sorption Isotherms Equations. Part I. Fruit, Vegetable and Meat Products*', Lebensmittel - Wissenschaft und Technologie, Vol. 18, N°2, pp. 111 - 117, 1985.

[13] R.R.H. Rizvi and A.L. Benado, '*Thermodynamics Properties of Dehydrated Foods*', *Food Technology*, Vol. 38, N°3, pp. 83 - 92, 1984.

[14] E. Akpinar, A. Midilli and Y. Bicer, '*Single Layer Drying Behaviour of Potato Slices in a Convective Cyclone Dryer and Mathematical Modelling*', Energy Conversion and Management, Vol. 44, N°10, pp. 1689 - 1705, 2003.

[15] M. Ozdemir and Y.O. Devres, '*The Thin Layer Drying Characteristics of Hazelnuts During Roasting*', Journal of Food Engineering, Vol. 42, N°4, pp. 225 – 233, 1999.

[16] J. Crank, '*Mathematics of Diffusions*', 2nd Ed., London: Oxford University Press, 1975.

[17] P.S. Madamba, R.H. Driscoll and K.A. Buckle, '*The Thin-Layer Drying Characteristics of Garlic Slices*', Journal of Food Engineering, Vol. 29, N°1, pp. 75 – 97, 1996.

[18] I. Doymaz, '*Drying Behaviour of Green Beans*', Journal of Food Engineering, Vol. 69, N°3, pp. 161 – 165, 2005a.

[19] I. Doymaz, '*Drying Characteristics and Kinetics of Okra*', Journal of Food Engineering, Vol. 69, N°3, pp. 275 – 279, 2005a.

[20] I. Doymaz, '*Convective Air Drying Characteristics of Thin Layer Carrots*', Journal of Food Engineering, Vol. 61, N°3, pp. 359 - 364, 2004.

[21] F. Kaymak-Ertekin, '*Drying and Rehydrating Kinetics of Green and Red Peppers*', Journal of Food Science, Vol. 67, N°1, pp. 168 - 175, 2002.

[22] W. Senadeera, B.R. Bhandari, G. Young and B. Wijesinghe, '*Influence of Shapes of Selected Vegetable Materials on Drying Kinetics during Fluidized Bed Drying*', Journal of Food Engineering, Vol. 58, N°3, pp. 277 - 283, 2003.

[23] S. Simal, A. Mulet, J. Tarrazo and C. Rosello, '*Drying Models for Green Peas*', Food Chemistry, Vol. 55, N°2, pp. 121 - 128, 1996.

[24] P.C. Panchariya, D. Popovic and A.L. Sharma, '*Thin-Layer Modelling of Black Tea Drying Process*', Journal of Food Engineering, Vol. 52, N°4, pp. 349 - 357, 2002.